Analyst

ROYAL SOCIETY OF CHEMISTRY

PAPER

View Article Online
View Journal | View Issue

Cite this: *Analyst*, 2021, **146**, 1281

Filter paper based SERS substrate for the direct detection of analytes in complex matrices†

Harmke S. Siebe, ‡[a] Qinglu Chen,‡[b] Xinyuan Li,[b] Yikai Xu, *[b] Wesley R. Browne [a] and Steven E. J. Bell *[b]

Surface-enhanced Raman spectroscopy (SERS) is an emerging analytical technique for chemical analysis, which is favourable due to its combination of short measurement time, high sensitivity and molecular specificity. However, the application of SERS is still limited, largely because in real samples the analyte is often present in a complex matrix that contains micro/macro particles that block the probe laser, as well as molecular contaminants that compete for the enhancing surface. Here, we show a simple and scalable spray-deposition technique to fabricate SERS-active paper substrates which combine sample filtration and enhancement in a single material. Unlike previous spray-deposition methods, in which simple colloidal nanoparticles were sprayed onto solid surfaces, here the colloidal nanoparticles are mixed with hydroxyethyl cellulose (HEC) polymer before application. This leads to significantly improved uniformity in the distribution of enhancing particles as the film dries on the substrate surface. Importantly, the polymer matrix also protects the enhancing particles from air-oxidation during storage but releases them to provide SERS enhancement when the film is rehydrated. These SERS-paper substrates are highly active and a model analyte, crystal violet, was detected down to 4 ng in 10 μL of sample with less than 20% point-by-point signal deviation. The filter paper and HEC effectively filter out both interfering micro/macro particles and molecular (protein) contaminants, allowing the SERS-paper substrates to be used for SERS detection of thiram in mud and melamine in the presence of protein down to nanogram levels without sample pre-treatment or purification.

Received 23rd October 2020,
Accepted 4th January 2021

DOI: 10.1039/d0an02103b

rsc.li/analyst

Introduction

Surface-enhanced Raman spectroscopy (SERS) has been extensively investigated as a technique for rapid chemical analysis which, due to its combination of short measurement time, high sensitivity and molecular specificity, could potentially exceed the performance of existing techniques at reasonable cost by exploiting affordable compact Raman spectrometers.[1–3] Current SERS substrates can be generally categorised into solid and liquid-based substrates. For on-site detection, solid substrates are convenient to use and are normally preferred over colloids, but they are typically more expensive to produce and/or present challenges with uniformity.[4–6] Conversely, assemblies of noble metal nanoparticles, in particular salt-aggregated Au and Ag colloids, are very widely used because they are simple to prepare and provide strong enhancement.[7] However, a fundamental problem with colloids is that they need to be aggregated, which is a dynamic process that eventually leads to nanoparticle precipitation. This means that with aggregated colloids there is a specific time window, normally within minutes, during which the optimal SERS enhancement can be achieved.[8,9] Other practical problems with colloids are that, even without addition of aggregating agents, they are inherently unstable and can be difficult to store. In addition, they require liquid handling procedures that are undesirable for field applications. As a result, their use has been largely limited to the study of pure samples in well-controlled laboratory settings.

We have previously addressed these issues by preparing solid substrates containing stable aggregates of Au and Ag nanoparticles which are held in a dry, protective polymer host. Specifically, addition of hydroxyethyl cellulose (HEC) to simple salt aggregated colloids creates a viscous solution, which can be subsequently dried into easy-to-handle free-standing films.[4,10,11] Importantly, in contrast to commonly used polymer capping agents, such as polyethylene glycol and polyvinylpyrrolidone,[12,13] HEC does not adsorb strongly onto the surface of the nano-

[a]*Stratingh Institute for Chemistry, University of Groningen, Nijenborgh 4, 9747 AG Groningen, The Netherlands*
[b]*School of Chemistry and Chemical Engineering, David Keir Building, Queen's University Belfast, BT9 5AG Belfast, Northern Ireland, UK. E-mail: yxu18@qub.ac.uk, s.bell@qub.ac.uk*

†Electronic supplementary information (ESI) available: SERS spectra, SEM, optical images. See DOI: 10.1039/d0an02103b

‡These authors contributed equally to this work.

particles. As a result, films can be reactivated by simply swelling the HEC with analyte dissolved in water or a range of other solvents. During the swelling process, the surfaces of the colloidal aggregates in the HEC films become exposed to the analyte, which can then adsorb onto them and be detected by SERS. Notably, the dry HEC matrix protects the particle aggregates from oxidation in storage and films have been shown to maintain 70% of their SERS activity even after one year.[4]

Here, we extend our previous work by developing a spraying method that allows SERS-active coatings, composed of nanoparticles stabilized in HEC, to be applied to solid supports of any size or shape. Since the material can be applied in much the same way as conventional paint (which also typically contains nanoparticles in a polymer binder), the process is both highly scalable and extremely flexible, so that a broad range of solid materials can be used as a support. Here we have illustrated the utility of the method by spraying coatings onto filter paper supports to create SERS-paper films. Since sample droplets can be applied to the reverse side of the substrate and are automatically filtered as they soak through the paper to reach the active particle layer, direct analysis of complex samples with micro/macro particulate contaminants, such as thiram in muddy water and melamine in protein solutions, is possible. Previous methods of introducing colloidal nanoparticles onto porous materials, such as filter paper,[14–17] nitrocellulose membranes[18] and polymer filter,[19–21] or adsorbent materials, such as ultra-thin chromatography boards,[22,23] allowed for sample filtering. However, since the nanoparticles in these substrates are exposed to air, they typically have a short shelf life ranging from hours to days.[24] As a result, these substrates must typically be freshly prepared prior to performing SERS analysis. In contrast, our method is a clear improvement, since the aggregates are protected by the encapsulating polymer, which means they retain their activity even if stored for extended periods. Moreover, the presence of the HEC polymer allows the nanoparticle aggregates to be deposited uniformly on the paper substrate, which has been extremely challenging for simple colloids dried onto solid supports.[25,26]

Experimental

Chemicals

Gold(III) chloride hydrate (>99%), sodium chloride (>99.5%, sodium citrate tribasic dihydrate (>99%), thiram (97%), crystal violet dye (anhydrous, ≥90.0%), albumin (98%), melamine (>99%), and Whatman filter paper were purchased from Sigma-Aldrich. Hydrochloric acid, nitric acid and hydroxyethyl cellulose were purchased from Honeywell Fluka. Milli-Q water (18.2 MΩ cm^{-1}) was used for all aqueous solutions. All glassware was cleaned with aqua regia then washed with Milli-Q water before use.

Preparation of SERS-paper films

In initial studies, hydroxylamine reduced silver colloid (HRSC) was prepared according to Leopold's method.[27] 48 mL of the colloid was concentrated by centrifugation to 15 mL. $MgSO_4$ (1.0 mL, 1.0 M) was used to pre-aggregate the colloid before adding HEC (96 mg, 0.6 w/v%). Mechanical stirring was used to obtain a homogeneous mixture, which was sprayed onto filter paper. All substrates for SERS studies were prepared using the following optimised method: HEC (0.31 g in 31 mL H_2O, 1 wt%) was dissolved in water overnight using a mechanical stirrer, forming a slightly viscous transparent solution. Citrate reduced gold colloid (CRGC) was prepared by the Turkevich method[28] and 48 mL of the colloid was concentrated by centrifugation to 9 mL. 1 mL of 1 M NaCl (aq.) was added to aggregate the colloid after which 10 mL of pre-dissolved HEC was added for stabilization. The mixture was stirred for 30 min before applying it to an airbrush. An ABEST dual action airbrush AB30 equipped with an ABEST air compressor AS186 was used to spray the HEC–CRGC mixture onto filter paper. A typical SERS substrate was obtained by spray-coating 5 × 20 mL of the HEC–CRGC mixture at an air pressure of 10 psi, with the outflow screw opened by 1 mm, which corresponded to a flow rate of 20 mL per hour. The distance between the airbrush and substrate was set at 32 cm. The polymer–colloid mixture was sprayed onto Whatman filter paper (∅ = 70 mm) grade 1 (pore size = 11 μm). The product SERS-paper substrate was cut into 5 × 5 mm^2 pieces using normal scissors and could be stored under dry conditions at room temperature.

Instrumentation

For SERS measurements 10 μL of analyte (aq.) were dried onto either the paper or the nanoparticle side of the substrate. Irrespective of which side the analyte was added onto, Raman spectra were always recorded from the nanoparticle side of the substrate. Samples of thiram in muddy water contained 0.08 g mL^{-1} of sand. Samples of melamine in protein solution contained 3 wt% albumin. SERS spectra were recorded using a PerkinElmer 785 nm Raman system equipped with a RamanMicro 200 microscope with a 10× objective lens, a spot size of 60 μm and power of 18 mW. SERS data were collected using an accumulation time of 20 s. SERS intensity maps were recorded using a WITec 785 nm Raman system, equipped with a 20× objective lens, with a laser power of 4 mW and a laser spot size of 2.4 μm. Areas of 25 μm × 25 μm were measured using 150 lines with 150 points per line and an accumulation time of 0.1 s per point. Scanning electron microscopy (SEM) images were recorded using a Quanta FEG 250 system at an acceleration voltage of 20 kV under high chamber pressure 1.15 × 10^{-5} mbar with standard copper tape as background. Atomic force microscopy (AFM) was conducted using a Nanosurf Flex AFM in dynamic force mode with Tap190Al-G cantilevers.

Results and discussion

Optimisation of SERS-paper films

Paper-based SERS substrates have previously been prepared by drop-casting colloids onto paper surfaces or by dip-coating

paper into colloids.[15–17,29,30] However, these methods typically lead to a very non-uniform distribution of nanoparticles on the substrate surface which results in relative standard deviations (RSD) of *ca.* 60%.[24] Conversely, it has been shown that spray-coating colloids onto paper surfaces can lead to much more uniform particle distributions, which significantly decreases the SERS RSD to *ca.* 20%.[24,31] Therefore, spray-coating was chosen here as the method of deposition (Fig. 1). Previous work performed using spray-coating to deposit nanoparticles onto filter paper surfaces used simple unaggregated colloids, which during the spraying process formed microdroplets of colloidal solution that dried almost immediately as random aggregated clusters on the surface of filter paper.[24,31,32] In this work, the nanoparticle solution needed to be pre-aggregated before HEC addition, since the nanoparticles are applied as a colloid–HEC polymer mixture in which the viscosity of the polymer hinders aggregation, even before evaporation and to a greater extent as the solution dries. Therefore, it was important to find the optimum concentration of aggregating agent and HEC polymer. Ideally, the colloid should be sufficiently aggregated to give strong SERS enhancement in the polymer solution, but remains well-dispersed throughout the polymer film rather than forming poorly dispersed large aggregates. It was found that, with the citrate reduced gold colloid (CRGC) used in this work, addition of 1 mL of 1 M NaCl (aq.) to 9 mL of concentrated colloid gave films with well-dispersed SERS particle clusters (see below).

The second set of experimental parameters to be optimised was the HEC concentration in the solution and the spraying conditions (distance from the target and spray rate). To minimise the spraying time, the polymer concentration was set at the highest value which still had a sufficiently low viscosity to allow the mixture to be sprayed. This concentration was determined by trial and error to be 1% w/w. In addition, to ensure the deposition of a uniform and strongly attached layer of HEC aggregates on the surface of the paper support, it is important to regulate the flow rate and the airbrush–paper distance. The latter parameter is important because the sprayed droplets will start to lose solvent as soon as they leave the spray nozzle and they need to reach the surface before drying completely, so that they are sufficiently wet to form a continuous film on the support's surface. The optimised airbrush–paper distance and air pressure conditions were found to be 32 cm and 10 psi, respectively (see Experimental for details).

Fig. 2A shows an example of a film sprayed onto a planar glass support, where an optical image under oblique illumination demonstrates that, although the deposited film is continuous and appears uniform under normal visual inspection, the surface is slightly uneven. However, the uniformity of the film is clearly better than other conventional methods, such as

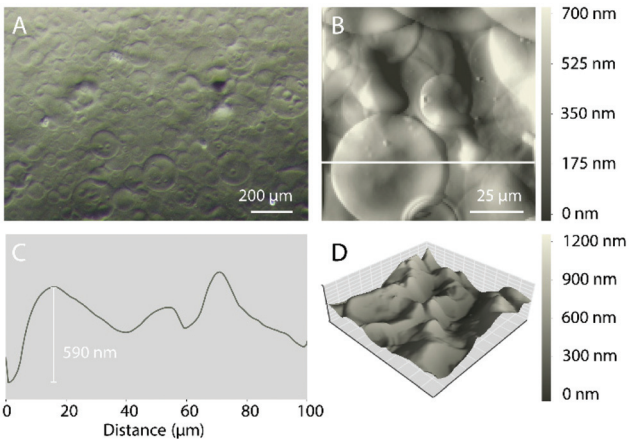

Fig. 2 A typical area of glass support covered with a 1 wt% HEC solution observed with an (A) optical and (B) atomic force microscope. (C) Line scan corresponding to the line in B, showing the height profile of the HEC on the surface of the glass substrate. (D) 3D view of the area in B.

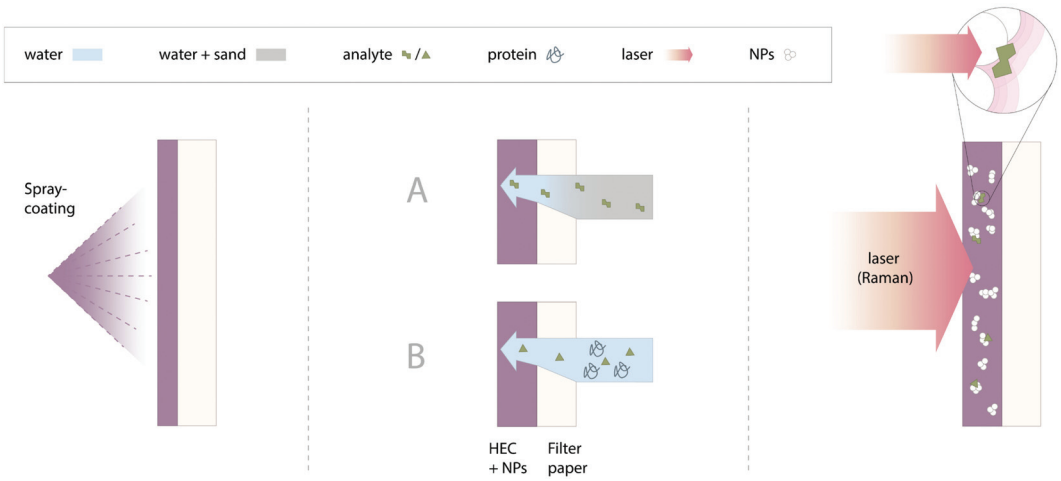

Fig. 1 Illustrations of (left) the substrate preparation by spray-coating, (middle) the filtration of analyte from (A) sand or (B) protein by application of sample on the paper side and (right) the detection of analyte on the nanoparticle side of the substrate using a Raman laser.

drop-casting, which dries into a very non-uniform nanoparticle coffee-ring.[21,26,33–35] The corresponding AFM images of the film on glass (Fig. 2B–D) indeed show that the film is not featureless but rather is composed of fused flatted disks <100 μm in diameter and <1 μm thick, which are the result of partly dried droplets sticking to the surface and then evaporating to dryness. Even at a fixed distance, the optimum spray rate depends on the substrate. For ease of preparation, the spray rate should be as high as possible, but it must be lower than the evaporation rate of the deposited droplets, otherwise the HEC–nanoparticle solution accumulates on the surface and finally drips off the support. This is less problematic on adsorbing supports such as paper or textiles where the solvent can wick into the material as well as evaporate from the surface.

Fig. 3 shows images of a piece of aggregated colloid–HEC paper (SERS-paper) produced under optimised experimental conditions. As shown in the optical image (Fig. 3A), the film is dark purple/grey which resembles the colour of the parent HEC aggregated CRGC (see Fig. S1†) and indicates that the plasmonic absorption of the aggregates is preserved throughout the spraying process. An illustration that the HEC–particle solution behaves like a paint coating is shown in Fig. 3B, which compares the SEM images of filter paper sprayed for different times. It is clear that the HEC gradually covers the cellulose fibres, filling in the voids between them until it forms a uniform film deposit. This was confirmed with SEM imaging of the cross-section of a piece of the SERS-paper film, as shown in Fig. S2.† Consistent with our AFM measurements discussed above, the SEM cross-section images showed that the HEC layer on the surface of the filter paper was lumpy and several hundreds of nm thick. Fig. 3C shows that on the tens of mm scale, the nanoparticles in the SERS-paper are distributed as randomly embedded clusters. Using high magnifications (Fig. 3D), the clusters were found to be composed of approximately 10–100 randomly assembled nanoparticles. As shown in Fig. S3,† the distribution and density of the clusters means that there are areas of ~500 nm^2 which are empty, this would result in some areas giving zero signal when the laser spot size used to record the SERS signal was of that order of magnitude. Here, however, the laser had a 60 μm diameter spot size, which is much larger than the size of the individual aggregates or the spaces between them, which meant that there were no blank areas and indeed the measured SERS signals were averaged from several thousand aggregates each time.

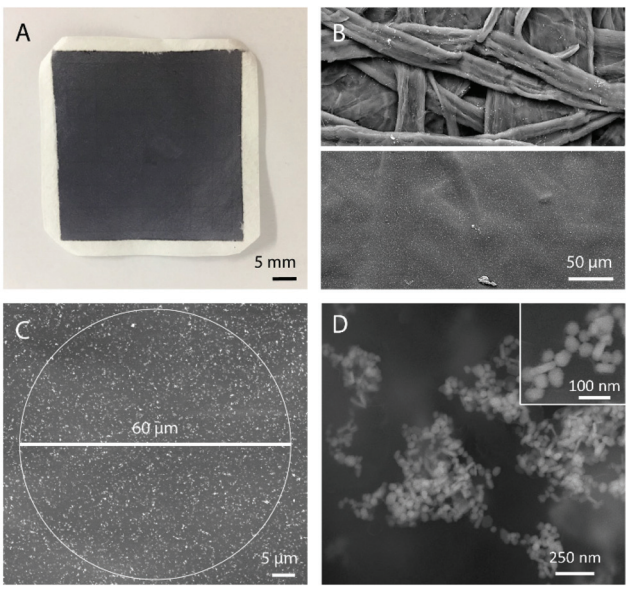

Fig. 3 (A) Optical image of a typical piece of SERS-paper. (B) (top) SEM images of filter paper sprayed with 16 mL of a concentrated aggregated HRSC in 0.6 wt% HEC solution and (bottom) 100 mL of the optimised SERS-paper 1 wt% HEC aggregated CRGC solution. (C) SEM image showing the distribution of nanoparticle aggregates within a 60 μm diameter laser spot in the SERS-paper substrate. (D) SEM image showing the aggregates in the HEC matrix of the SERS-paper at high magnification.

Determination of the SERS properties of the SERS-paper films

Fig. 4 shows the SERS signature of a typical SERS-paper film. The spectrum is dominated by a band at 268 cm^{-1}, which corresponds to the Au–Cl vibration arising from the adsorbed monolayer of chloride ions on the surface of the gold aggregates. Interestingly, although the gold aggregates were embedded directly in HEC, the polymer did not give rise to observable Raman bands in the SERS spectra, suggesting that, although the polymer surrounds the aggregates, it does not penetrate into the nanogap "hot spots" between the particles during the drying process. The SERS uniformity and batch-to-batch reproducibility of the sprayed films was characterised by two different samples of SERS-paper films prepared as *ca.* 1225 mm^2 sheets, which were divided into ≥30 pieces (*ca.* 25 mm^2 in size). The intensity of the Au–Cl vibration, monitored on five different spots on each piece, is shown in Fig. 5, where the RSD in average signal intensities was found to be 19.1% and 20.0% in substrate A and B, respectively. This is

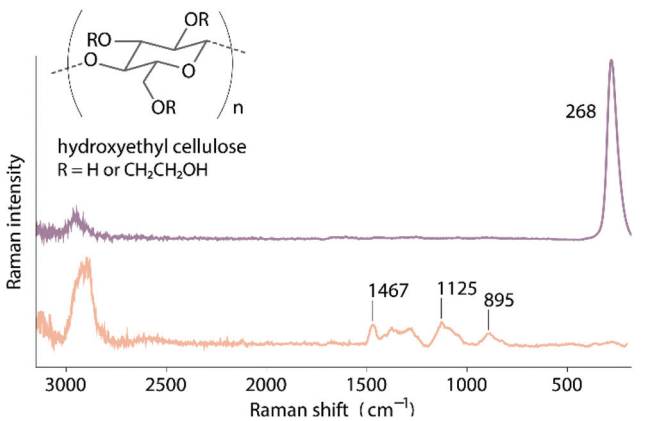

Fig. 4 SERS spectrum of the nanoparticle side of the SERS-paper film (purple). Raman spectrum of HEC powder (orange). The spectra are scaled for comparison.

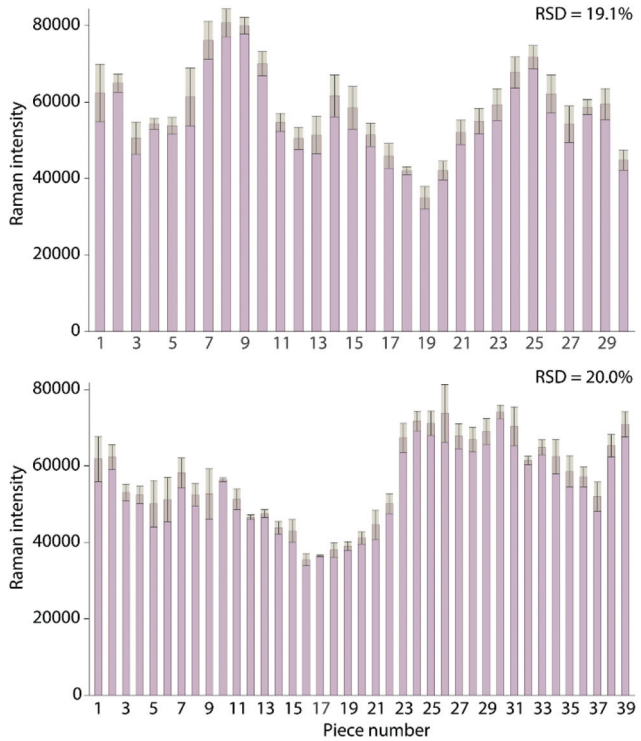

Fig. 5 SERS intensity of the 268 cm^{-1} band in each of the pieces cut from prepared films A (top) and B (bottom). Each data point represents the average value from five SERS spectra and error bars show the RSD. The RSD of the average values were 19.1% for film A and 20.0% for film B.

comparable to the RSD reported for other sprayed SERS substrates in literature[23,24,31,32] and superior to the RSD of paper SERS substrates fabricated through dip-coating.[24] Moreover, the average signal intensities between the two batches of SERS-paper only differed by 3%, which demonstrates the high reproducibility of the spray-coating approach.

Interaction of SERS-paper films with analyte solutions

While the uniformity test above gives a good indication of the distribution of enhancing particles in the dry films, it is important to note that in use the analyte will be applied as a liquid droplet, which swells the film before drying down onto the particles and could potentially give rise to inhomogeneous drying effects. Therefore, further uniformity tests were carried out using crystal violet (CV) as analyte. Initial tests applying droplets of various CV concentrations to the nanoparticle side of the film and drying the sample, showed that the intensity of the signals grew in the conventional manner, starting from a concentration of 10^{-6} M (4 ng of analyte in 10 μL sample) with a smooth increase in intensity up to the saturation concentration at *ca.* 5×10^{-5} M, above which the signal plateaued as the enhancing surface became saturated (Fig. 6A). Representative SERS spectra of 10 μL of 10^{-5} M CV dried on the nanoparticle and paper side of the substrate are shown in Fig. 6B. The SERS spectra were always recorded from the nanoparticle side, no matter on which side the sample was applied. A concentration of 10^{-4} M, which was just above the saturating concentration, was used for a uniformity test. Fig. 6C shows the Raman intensity maps of the CV band at 1172 cm^{-1} measured over a 25 μm × 25 μm area of an analyte droplet dried on the nanoparticle and the paper side of the substrate (see also Fig. S4 and 5†). The SERS signal of CV was found to be relatively constant in both cases. Notably, there was no evidence of the local high intensity regions that are characteristic of the coffee-rings which are often observed on solid SERS substrates.

Interestingly, the RSD of the SERS signal of CV deposited on the nanoparticle side of the substrate was *ca.* 9.8%, which

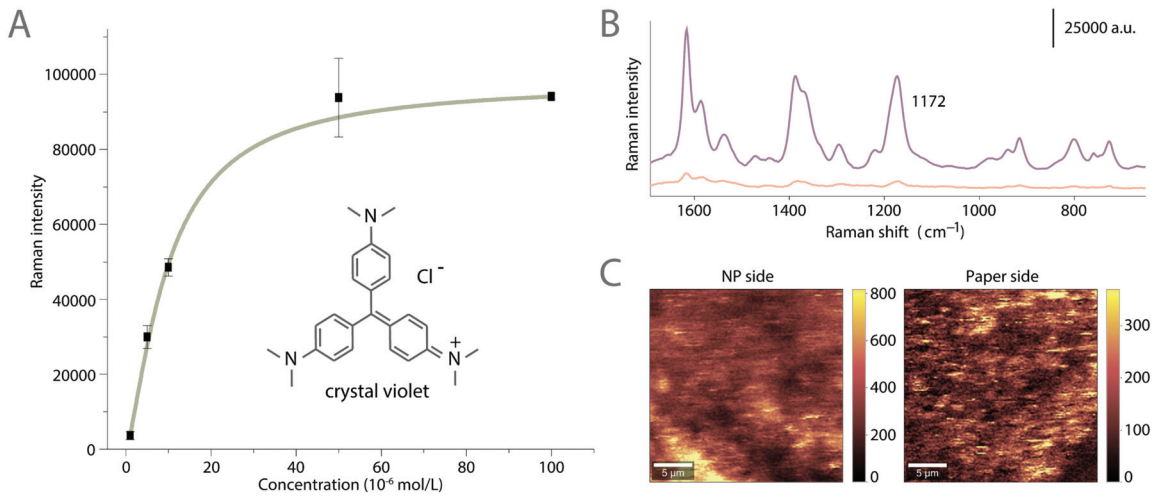

Fig. 6 (A) SERS intensity of the 1172 cm^{-1} band of CV dried on the nanoparticle side of the substrate at different concentrations. Data points are an average over 5 measurements and error bars represent the SD. (B) SERS spectra obtained from drying 10 μL of 10^{-5} M CV solution onto the nanoparticle (purple) and paper (orange) side of the SERS-paper film. (C) Intensity maps of the 1172 cm^{-1} band of an area of 25 μm × 25 μm of a droplet of 10 μL 10^{-4} M CV dried on the nanoparticle (left) and paper (right) side of the SERS-paper film.

is smaller than the *ca.* 20% value of the parent film. It is possible that this is due to redistribution of the enhancing aggregates during the swelling/redrying process, causing further randomisation of the location of the enhancing particle clusters, which reduces the point-to-point variability of the film. Of course, the more interesting test was that where the sample was applied to the paper side of the film, since this is required if the paper is to act as a filter for analysing complex samples. Since the CV solution should be free to penetrate the paper and swell the polymer, it was expected that similar intensity signals of CV would be observed irrespective of the side that CV was applied to. In fact, it was clear that CV was significantly impeded by the intervening filter paper layer, as a 10^{-5} M test solution, which gave *ca.* 50 000 cts when applied to the polymer–nanoparticle face, gave a signal of just 5000 cts when applied to the paper side (Fig. 6B). Clearly, the paper layer hindered the access of adsorbing dyes to the enhancing layer on the reverse face. Hence, the films can be used as filters which can select against molecules that adsorb to the paper fibres and thereby prevent them from penetrating through to the enhancing nanoparticle layer.

Detection of analytes in complex solutions

While the test experiments with CV discussed above are promising, our main objective is detecting analytes of interest while simultaneously excluding interfering materials. This is because the samples in many real-life field-testing applications are not clean aqueous solutions, but rather complex mixtures. These mixtures contain components such as suspended micro/macro particles, which cause turbidity, or molecular contaminants that can compete for the enhancing nanoparticle surface. Here we have chosen two simple test systems to investigate the potential of our SERS substrate for combining direct analysis with removal of interfering components from contaminated samples.

The first test analyte chosen was thiram, which is a representative of sulfur-based organic fungicides that are potential toxic pollutants in water and soil.[36] Thiram has a strong affinity for noble metal nanoparticles because it contains a disulfide functional group. This high affinity allowed it to be detected down to 10^{-7} M (*ca.* 0.24 ng total analyte in 10 μL sample) when applied as a pure aqueous solution to the nanoparticle side of the SERS-paper films (Fig. S6†). However, when a droplet of thiram solution in water which was contaminated by sand to represent a soil sample, was applied directly onto the nanoparticle side of the sprayed films, the sand particles masked the enhancing aggregates from the laser light. As a result, SERS signals of thiram were not observed, even at high (10^{-4} M) concentrations (Fig. S7†). In contrast, when the contaminated solution was introduced from the filter paper side of the sprayed films, the solid particulates were filtered from the solution but the strong thiram signals were retained. Indeed, as shown in Fig. 7, the response of the SERS-paper film to the clean and sandy thiram solutions was almost identical. The slopes of the linear calibration plots over the 10^{-6} M to 10^{-4} M concentration range differed by <1%. Impressively,

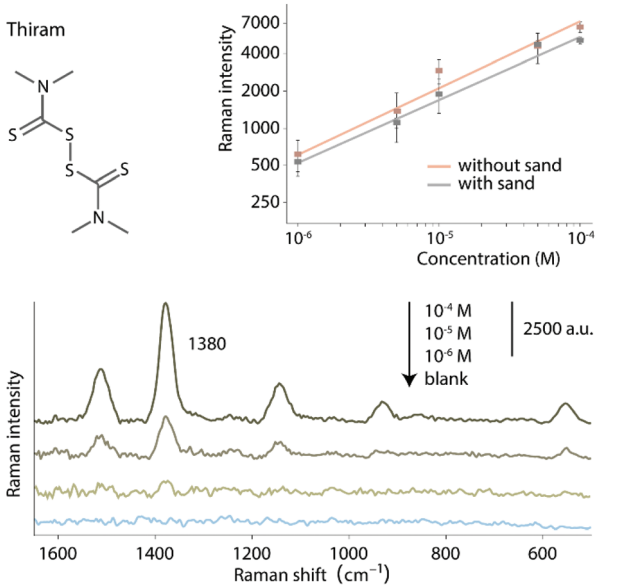

Fig. 7 SERS intensity of different concentrations of aqueous thiram solutions with (grey) and without (orange) sand contamination, both applied from the paper side of the SERS-paper. Data points are an average over 5 measurements and error bars represent ±1 SD. Lines are obtained using a best fit log function (top). The SERS spectra of several solutions of thiram contaminated with sand applied to the paper side of the substrate show the detection limit of 10^{-6} M (bottom).

even for the contaminated samples, the correlation coefficient of the calibration line was >0.98 over the linear calibration range.

The second test analyte chosen was melamine, a nitrogen-rich compound which has been illegally added to milk to increase the apparent protein content, a practice which has led to infant deaths.[37] Melamine can spontaneously adsorb to noble metal nanoparticle surfaces and in pure aqueous solution was detected down to 10^{-4} M (*ca.* 126 ng) and 5×10^{-5} M (*ca.* 63 ng) when applied from the paper and nanoparticle side of the SERS-paper films, respectively (Fig. S8†). However, in milk samples the large number of strongly adsorbing protein molecules compete with melamine for surface sites, making SERS detection of melamine in milk very challenging. As a result, various methods to remove or deactivate the protein prior to SERS analysis have been developed.[38–40] However, as shown in Fig. 8, strong melamine signals could be directly detected for melamine/albumin solutions using SERS-paper films. When the sample was applied to the paper side of the substrate, the detection limit of melamine (calculated as the point where signal = $3\sigma s \sim 3 \times 150$ cts s^{-1}) was 5×10^{-5} M (*ca.* 63 ng), the same as when there was no protein present, showing the effectiveness of film in filtering albumin. Using the most intense sample band at 706 cm^{-1}, the linear quantification range was from 10^{-5} M to 10^{-2} M with an R^2 of 0.97. Interestingly, it was found that SERS signals of melamine could also be detected when the melamine/albumin solution was applied directly from the nanoparticle side of the films

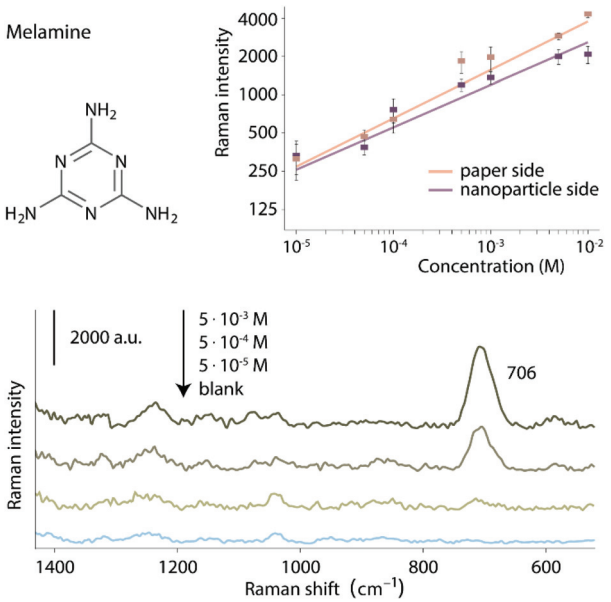

Fig. 8 SERS intensity of different concentrations of aqueous melamine solutions with albumin applied from the paper (orange) or the nanoparticle (purple) side of the SERS-paper. Data points are an average over 5 measurements and error bars represent the SD. Lines are obtained using a best fits log function (top). The SERS spectra of several solutions of melamine contaminated with albumin applied to the paper side of the substrate show the detection limit of 5×10^{-5} M (bottom).

and that the signals were very similar to those obtained from the paper side. It has been shown that protein molecules have a strong affinity towards HEC.[29] This suggests that within the SERS-paper the HEC matrix can act as a molecular filter to remove proteins and it is this effect which allows melamine to be analysed directly in protein solutions. In this case, the paper support plays only a minor role in preventing interference by the protein, although the slightly larger signals observed for high concentration solutions when the sample is introduced from the paper side, suggests it does give a detectable improvement.

The detection of analytes such as thiram and melamine in real-life samples carried out under laboratory conditions normally involves complex sample clean-up steps and use of expensive equipment, such as liquid chromatography-mass spectroscopy systems that combine separation and detection.[41,42] Although this allows extremely low concentrations (sub-nanomolar) of analyte to be detected, it is expensive and time consuming. In contrast, the SERS-paper films allow samples present in complex environments to be detected directly, without sample preparation, within seconds using inexpensive materials and instruments. For both thiram and melamine the limit of detection is higher than is possible for conventional chromatographic analysis but, critically, is below the lethal concentration level of thiram in fish/rats[43,44] and the amount of melamine found in the contaminated milk powder incidents in China,[45] respectively.

Conclusion

Rapid and inexpensive methods for sensitive and quantitative detection of chemical compounds in complex matrices are significant for a variety of applications. While SERS offers a potential solution to this problem, developing methods to fabricate substrates which provide the appropriate balance of enhancing properties and cost effectiveness is challenging. In this work, we present a cost effective and scalable spray-coating method to fabricate SERS-paper substrates with the combined ability of sample clean-up and Raman signal enhancement. In contrast to conventional methods, in which exposed nanoparticles are deposited onto substrate surfaces, our method involves spraying plasmonic nanoparticles mixed with solubilised HEC polymer. When dry, this polymer forms a protective matrix around the enhancing particles, thereby significantly hindering oxidation of the enhancing noble metal nanoparticle aggregates. Upon contact with aqueous solutions, however, the polymer rehydrates and swells and activates the enhancing properties of the embedded nanoparticle aggregates. Even with simple aggregated citrate-reduced gold nanoparticles as the plasmonic component, the SERS-paper films were highly active and allowed detection of crystal violet (CV) down to 4 ng in 10 μL of sample. Moreover, the HEC matrix and paper support combine to act as a filter, which removes competing molecules and light scattering particulate contaminants that otherwise interfere with analysis. This allowed samples of thiram in muddy water and melamine in solutions containing albumin to be directly and quantitatively detected down to ng levels. The spray-coating method developed in this work can be potentially combined with a conveyer-belt setup for industrial scale production of SERS substrates, which, when combined with portable Raman spectrometers, offers a cheap, rapid, convenient and sensitive approach for on-site chemical analysis.

Author contributions

H. S. S. contributed to data curation, formal analysis, investigation, methodology development, visualisation, writing-original draft. Q. C. contributed to data curation, formal analysis, investigation, methodology development, visualisation. X. L. contributed to data curation, formal analysis, investigation. Y. X. contributed to conceptualisation, data curation, formal analysis, project administration, supervision, validation, writing-review and editing. W. R. B. contributed to funding acquisition, supervision, writing-review and editing. S. E. J. B. contributed to conceptualisation, formal analysis, funding acquisition, resources, supervision, validation, writing-review and editing.

Conflicts of interest

There are no conflicts to declare.

Acknowledgements

H. S. S. acknowledges The Netherlands Ministry Culture and Science (Gravity Program 024.001.035) for financial support. Y. X acknowledges a University Special Research Scholarship (Q. U. B.) and a Leverhulme Trust Early Career Fellowship for Financial support.

Notes and references

1 M. Eryılmaz, E. A. Soykut, D. Çetin, İ. H. Boyacı, Z. Suludere and U. Tamer, *Analyst*, 2019, **144**, 3573–3580.
2 N. A. Owens, L. B. Laurentius, M. D. Porter, Q. Li, S. Wang and D. Chatterjee, *Appl. Spectrosc.*, 2018, **72**, 1104–1115.
3 P. A. Mosier-Boss, *Nanomaterials*, 2017, **7**, 142.
4 W. W. Y. Lee, V. A. D. Silverson, C. P. McCoy, R. F. Donnelly and S. E. J. Bell, *Anal. Chem.*, 2014, **86**, 8106–8113.
5 F. Wieduwilt, C. Lenth, G. Ctistis, U. Plachetka, M. Möller and H. Wackerbarth, *Sci. Rep.*, 2020, **10**, 8260.
6 W. W. Yu and I. M. White, *Anal. Chem.*, 2010, **82**, 9626–9630.
7 B. Sharma, R. R. Frontiera, A.-I. Henry, E. Ringe and R. P. Van Duyne, *Mater. Today*, 2012, **15**, 16–25.
8 R. Tantra, R. J. C. Brown and M. J. T. Milton, *J. Raman Spectrosc.*, 2007, **38**, 1469–1479.
9 S. Sánchez-Cortés, J. V. Garcıa-Ramos and G. Morcillo, *J. Colloid Interface Sci.*, 1994, **167**, 428–436.
10 W. W. Y. Lee, V. A. D. Silverson, L. E. Jones, Y. C. Ho, N. C. Fletcher, M. McNaul, K. L. Peters, S. J. Speers and S. E. J. Bell, *Chem. Commun.*, 2016, **52**, 493–496.
11 W. W. Y. Lee, C. P. McCoy, R. F. Donnelly and S. E. J. Bell, *Anal. Chim. Acta*, 2016, **912**, 111–116.
12 J. Manson, D. Kumar, B. J. Meenan and D. Dixon, *Gold Bull.*, 2011, **44**, 99–105.
13 K. M. Koczkur, S. Mourdikoudis, L. Polavarapu and S. E. Skrabalak, *Dalton Trans.*, 2015, **44**, 17883–17905.
14 M.-L. Cheng, B.-C. Tsai and J. Yang, *Anal. Chim. Acta*, 2011, **708**, 89–96.
15 C. Wang, B. Liu and X. Dou, *Sens. Actuators, B*, 2016, **231**, 357–364.
16 P. Rajapandiyan and J. Yang, *J. Raman Spectrosc.*, 2014, **45**, 574–580.
17 W.-L.-J. Hasi, X. Lin, X.-T. Lou, S. Lin, F. Yang, D.-Y. Lin and Z.-W. Lu, *Appl. Phys. A*, 2015, **118**, 799–807.
18 A. G. Berger, S. M. Restaino and I. M. White, *Anal. Chim. Acta*, 2017, **949**, 59–66.
19 S. Fateixa, M. Raposo, H. I. S. Nogueira and T. Trindade, *Talanta*, 2018, **182**, 558–566.
20 W. Y. Wei and I. M. White, *Analyst*, 2012, **137**, 1168–1173.
21 W. Wang, Y. Yin, Z. Tan and J. Liu, *Nanoscale*, 2014, **6**, 9588–9593.
22 J. Chen, Y.-W. Huang and Y. Zhao, *J. Mater. Chem. B*, 2015, **3**, 1898–1906.
23 Z.-M. Zhang, J.-F. Liu, R. Liu, J.-F. Sun and G.-H. Wei, *Anal. Chem.*, 2014, **86**, 7286–7292.
24 B. Li, W. Zhang, L. Chen and B. Lin, *Electrophoresis*, 2013, **34**, 2162–2168.
25 M. Lee, K. Oh, H.-K. Choi, S. G. Lee, H. J. Youn, H. L. Lee and D. H. Jeong, *ACS Sens.*, 2018, **3**, 151–159.
26 R. Ambroziak, J. Krajczewski, M. Pisarek and A. Kudelski, *ACS Omega*, 2020, **5**, 13963–13972.
27 N. Leopold, M. Haberkorn, T. Laurell, J. Nilsson, J. R. Baena, J. Frank and B. Lendl, *Anal. Chem.*, 2003, **75**, 2166–2171.
28 J. Turkevich, P. C. Stevenson and J. Hillier, *Discuss. Faraday Soc.*, 1951, **11**, 55–75.
29 F. Zeng, T. Mou, C. Zhang, X. Huang, B. Wang, X. Ma and J. Guo, *Analyst*, 2019, **144**, 137–142.
30 X. Lin, S. Lin, Y. Liu, H. Zhao, B. Liu and L. Wang, *J. Raman Spectrosc.*, 2019, **50**, 916–925.
31 A. Bolz, U. Panne, K. Rurack and M. Buurman, *Anal. Methods*, 2016, **8**, 1313–1318.
32 W. Jang, H. Byun and J.-H. Kim, *Mater. Chem. Phys.*, 2020, **240**, 122124.
33 J. Cailletaud, C. De Bleye, E. Dumont, P.-Y. Sacré, Y. Gut, L. Bultel, Y.-M. Ginot, P. Hubert and E. Ziemons, *Talanta*, 2018, **188**, 584–592.
34 Y. Hong, Y. Li, L. Huang, W. He, S. Wang, C. Wang, G. Zhou, Y. Chen, X. Zhou, Y. Huang, W. Huang, T. Gong and Z. Zhou, *J. Biophotonics*, 2020, **13**, e201960176.
35 C. Miccichè, G. Arrabito, F. Amato, G. Buscarino, S. Agnello and B. Pignataro, *Anal. Methods*, 2018, **10**, 3215–3223.
36 M. Couderchet, *Vitis*, 2003, **42**, 165–172.
37 A. K.-c. Hau, T. H. Kwan and P. K.-t. Li, *J. Am. Soc. Nephrol.*, 2009, **20**, 245–250.
38 F. Sun, H.-C. Hung, A. Sinclair, P. Zhang, T. Bai, D. D. Galvan, P. Jain, B. Li, S. Jiang and Q. Yu, *Nat. Commun.*, 2016, **7**, 1–9.
39 S. S. Panikar, G. Ramírez-García, S. Sidhik, T. Lopez-Luke, C. Rodriguez-Gonzalez, I. H. Ciapara, P. S. Castillo, T. Camacho-Villegas and E. De la Rosa, *Anal. Chem.*, 2018, **91**, 2100–2111.
40 A. Vicario, V. Sergo, G. Toffoli and A. Bonifacio, *Colloids Surf., B*, 2015, **127**, 41–46.
41 V. K. Sharma, J. S. Aulakh and A. K. Malik, *J. Environ. Monit.*, 2003, **5**, 717–723.
42 Y. Liu, E. E. D. Todd, Q. Zhang, J.-r. Shi and X.-j. Liu, *J. Zhejiang Univ., Sci., B*, 2012, **13**, 525–532.
43 S. Babo and P. Vasseur, *Aquat. Toxicol.*, 1992, **22**, 61–68.
44 B. Rai and S. D. Mercurio, *Environ. Sci. Pollut. Res.*, 2020, **27**, 10629–10641.
45 C. M.-E. Gossner, J. Schlundt, P. B. Embarek, S. Hird, D. Lo-Fo-Wong, J. J. O. Beltran, K. N. Teoh and A. Tritscher, *Environ. Health Perspect.*, 2009, **117**, 1803–1808.

